Biosensors and Bioelectronics 192 (2021) 113528

Contents lists available at ScienceDirect

Biosensors and Bioelectronics

journal homepage: www.elsevier.com/locate/bios

Photoelectrochemical aptasensor based on $La_2Ti_2O_7/Sb_2S_3$ and V_2O_5 for effectively signal change strategy for cancer marker detection

Rui Xu [a], Yu Du [a,*], Hongmin Ma [a], Dan Wu [a], Xiang Ren [a], Xu Sun [a], Qin Wei [a], Huangxian Ju [a,b]

[a] Collaborative Innovation Center for Green Chemical Manufacturing and Accurate Detection; Key Laboratory of Interfacial Reaction & Sensing Analysis in Universities of Shandong, School of Chemistry and Chemical Engineering, University of Jinan, Jinan, 250022, PR China
[b] State Key Laboratory of Analytical Chemistry for Life Science, School of Chemistry and Chemical Engineering, Nanjing University, Nanjing, 210023, China

ARTICLE INFO

Keywords:
$La_2Ti_2O_7$
Sb_2S_3
V_2O_5
On-off-on
PEC aptasensor

ABSTRACT

In this item, a high-efficiency signal "on-off-on" strategy photoelectrochemical (PEC) apatsensor was resoundingly developed for target ultrasensitive analysis. Primarily, the heterojunction formation between Cd: Sb_2S_3 and $La_2Ti_2O_7$ was contributed to the first "signal-on" state to improve the stability of the PEC platform. Secondly, V_2O_5 nanosphere act as a catalyst for H_2O_2 was used to label on aptamer DNA to consume electron donor for achieving "signal-off" state. Then target analyte was modified on the surface of the PEC platform, and part of V_2O_5 with aptamer DNA would be released from the aptasensor surface, thus, the "signal-on" state was realized again. In this signal "on-off-on" strategy, the PEC performance of perovskite $La_2Ti_2O_7$ was effectively perfected with Cd: Sb_2S_3 sensitization, and broaden the application of perovskite in PEC sensor field. And the signal attenuation and recovery strategy were distinctly elevated the sensitivity of the aptasensor. In the preferred detection conditions, the proposed PEC sensor for analyte (PSA as an example) analysis revealed a wide sensing range from 1.000×10^{-5} to 500.0 ng/mL, own a low detection limit of 4.300 fg/mL. This smart response change mode also provide prospect for other target detection, and offer a reference to signal transform for other electrochemical method.

1. Introduction

In recent years, electrochemical sensing analysis is received wide attention in various kind of target detection, and the increasement demands are required. Photoelectrochemical (PEC) as a branch of electrochemical is developed rapidly because its unique signal conversion way and attractively sensitivity (Huang et al. 2018, 2019; Zhu et al., 2019). However, due to the single signal change trend, some unignored drawbacks such as the background signals is still existed. As an effective method for ultrasensitive determination, the "on-off-on" strategy has been widely adopted in biomarker determination (Huang et al., 2017; Kong et al., 2018; Li et al., 2016), which can availably get out of the defects of the "signal on" and "signal off" mode (Huang et al., 2013; Wang et al. 2010, 2018; Ye et al., 2017). Herein, a PEC aptasenor depend on the signal "on-off-on" mode was designed for target super-sensitivity detection.

Accordingly, perovskite oxides (ABO_3) are more attractive than simple oxides as photoelectrode in PEC analysis (Liang et al., 2020; Wang et al., 2019), which is due to their high activity and excellent compositional and structural flexibility, offering the possibilities to achieve high photoelectrochemical stability, super visible light absorption capacity (Ruan et al., 2017), and accurate control band gaps and edges simultaneously (Liu et al., 2017; Nassar et al., 2018; Wang et al., 2017a). As a kind of perovskite oxides, $La_2Ti_2O_7$ possess a strong reduction-oxidation ability which was used in this work to produce the basis photocurrent (Bin Adnan et al., 2018; Wan et al., 2018; Wang et al., 2017b), but the visible light capturing efficiency was limited by the wide band gap (about 3.4 eV) (Zhang et al., 2018b), while the "on-off-on" strategy need a high enough original photocurrent to support the stability and sensitivity. Fortunately, Sb_2S_3 has become a fresh light-absorbing material with great stability in surroundings (Lu et al., 2017), excellent absorptivity in visible light range, and rich elemental storage (Chen et al., 2018; Tang et al., 2018). It could load on $La_2Ti_2O_7$ surface to form the heterojunction, and offered a higher photocurrent resultful owing to the matched band energy level. Besides, Cd^{2+} was dopped in Sb_2S_3 which could prefer the band gap of Sb_2S_3 (the band gap of Cd: Sb_2S_3 is shown in Fig. S1), and narrow the energy level gradient with $La_2Ti_2O_7$, thus further boosting the electron transfer. Under the

* Corresponding author.
E-mail addresses: XuRui19950218@163.com (R. Xu), duyu_ujn@163.com (Y. Du).

https://doi.org/10.1016/j.bios.2021.113528
Received 22 March 2021; Received in revised form 24 June 2021; Accepted 20 July 2021
Available online 21 July 2021

combined effect of these two favorable photoactive materials, the first "signal-on" state was achieved.

Besides the satisfactory enhanced original photocurrent, the useful quencher is also crucial to lower the background response, and further enhance the sensitivity. V_2O_5 nanospheres owns great electrical and thermal stability, low cost, and easy availability (Ghosh et al., 2018) which was used to label on aptamer DNA (aDNA) to catalyzed H_2O_2 (electron donor) (André et al., 2011; Hu et al., 2014; Yang et al., 2018; Zhang et al., 2019). During the processes of the aptasensor construction, both non-conductivity and steric hindrance could decrease the PEC signal, after the modification of V_2O_5, the electron donor was catalyzed, and the photocurrent would be decreased sharply. Thus, the preferred "signal-off" state was realized, and the magnifying signal changed value further improved the sensitivity of the sensor. At the same time, when the target molecule (PSA as an example analyte) was touched on the surface of aptasensor, part of the aDNA-V_2O_5 was specific recognized with the target, and released from the photoelectrode, thus resulting in the "signal-on" state again.

Herein, a skillful signal "on-off-on" PEC aptasensor was designed to PSA supersensitive detection. The PEC basic material used Cd: Sb_2S_3 sensitized light-stable perovskite $La_2Ti_2O_7$, which is modified on the gold-deposited photoelectrode. The sensitization of Cd: Sb_2S_3 polished the poor photocatalytic performance of perovskite and widened its application in PEC field. Then, the capture DNA (cDNA) and aDNA-V_2O_5 was linked on the photosensitive electrode via the cross-linking agent to contributed the super-sensitivity performance. Finally, the target PSA was decorated to realize quantitative detection rely on the gradually re-increased photocurrent. The PEC aptasensor fabrication process is shown in Scheme 1.

2. Experimental section

2.1. Preparation of $La_2Ti_2O_7$ nanosheets

The $La_2Ti_2O_7$ nanosheets was prepared via s simple hydrothermal reaction (Wang et al., 2017b). 4.331 g of $La(NO_3)_3{\cdot}6H_2O$ and 2.342 g of $Ti(SO_4)_2$ was dissolved into 60 mL of ultrapure water under continues stirring. Then, 20 mL of NaOH solution (0.1 M) was added to the mixture and stirring violently. After 15 min, the solution was poured into a dry 100 mL Teflon-lined autoclave, maintain at 200 °C for a whole day and obtained the white sediment, the product was washed for several times with ultrapure water, later dried at 80 °C.

2.2. Synthesis of V_2O_5 nanosphere

The preparation of V_2O_5 nanosphere was performed via a two-step method (Zou et al., 2016). First, 0.7019 g of NH_4VO_3 was dispersed in 135 mL of ultrapure water with stirring for 15 min. After that, 3 mL of HCl (1 M) was added in the solution, and the solution was changed to yellow. Then, 9 mL of hydrazine hydrate was added and kept stirring for 2 h. After the color of solution changed to gray, the precipitate was rinsed with ethyl alcohol and ultrapure water, later dried at 60 °C overnight. Finally, the obtained product was calcined at 350 °C for 2 h to get the yellow V_2O_5 nanosphere.

2.3. Preparation of aDNA-V_2O_5

Firstly, the as-prepared V_2O_5 nanosphere was functional with amino. Then 500 μL of aDNA (1 μM) solution was added into 2 mL of amino-functionalized V_2O_5 (V_2O_5–NH_2, 10 mg/mL) solution, the mixture was incubated at 37 °C for an hour, and then washed with PBS buffer solution (pH 7.4). After that, the product was dispersed in 1 mL PBS buffer solution containing with 100 μL of BSA (1 %), and further incubated at 37 °C for an hour, then washed with PBS solution for one time. Finally, the product was dispersed in the PBS solution once again, and stored in a refrigerator at 4 °C for later use. Other details of materials preparation are displayed in *Supplementary Material* (SM) file.

2.4. Fabrication of PEC aptasensor

The signal "on-off-on" PEC aptasensor was designed on the Indium Tin Oxide (ITO) glass electrode via the layer by layer drop coating way. Previous modification processes, the ITO glass was cut into a size of 2 × 0.8 cm^2, and ultrasonic cleaning with detergent, acetone, ethanol, and water in turn. First of all, the ITO electrode was performed with electrodeposition gold to obtained a more stable PEC platform. Then, the photoactive materials of $La_2Ti_2O_7$ (10 μL, 6 mg/mL) and Cd: Sb_2S_3 (6 μL, 4 mg/mL) were dropped on the electrode successively. After dried naturally, 6 μL of EDC-NHS mixture solution (the concentration of EDC and NHS are 5 mg/mL and 1 mg/mL) and NH_2-cDNA (6 μL, 1 μM) was modified on the electrode, and allowed incubate at 4 °C. Then the photoelectrode was carefully cleaned with PBS buffer solution, MCH was modified to block the inactive sites. Follow that, 6 μL of aDNA-V_2O_5 solution was modified on the photoelectrode and incubated. Finally, various concentrations of PSA were decorated on the washed PEC platform and washed after incubated 40 min. Hereto, the sensitive PEC aptasensor was realized.

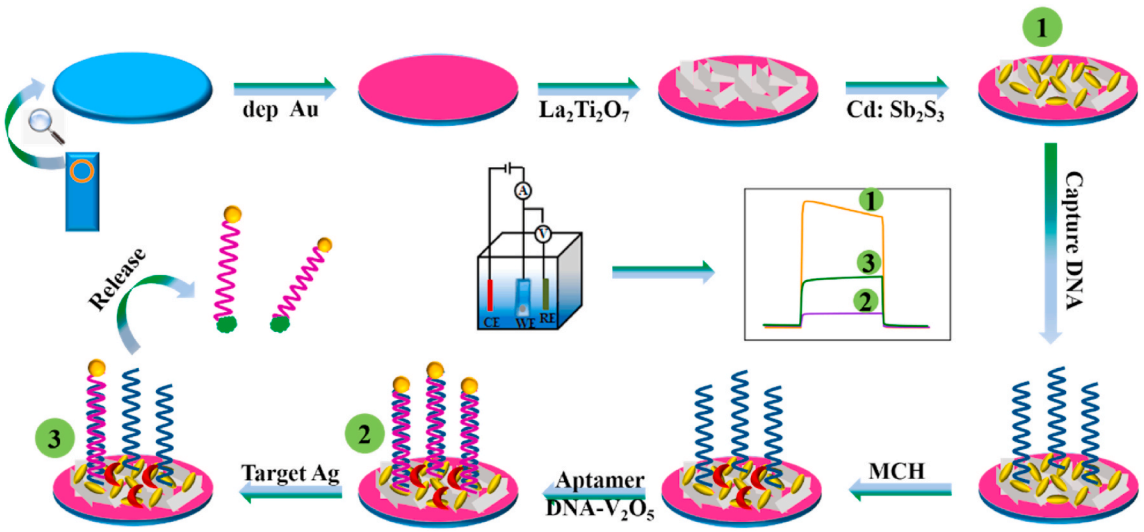

Scheme 1. The fabrication processes of the aptasensor.

2.5. PEC determination

The PEC response measurement was carried out in 10 mL of PBS buffer solution containing with suitable concentration of H_2O_2 (electron donor). The fabrication PEC aptasensor supported on ITO photoelectrode was act as the work electrode, and the column platinum electrode act as the auxiliary electrode while Ag/AgCl electrode was act as the reference electrode. The light source was powered by xenon lamp with wavelength greater than 400 nm, the light was turn on and off at intervals of 10 s each cycle, and there is no extra bias voltage.

3. Experimental results and discussion

3.1. Materials characterization

As the foundation of the PEC aptasensor, basic photoactive materials were analyzed and characterized firstly, X-ray diffraction (XRD) was used to qualitative analysis of materials. Fig. 1A shows XRD analysis of the perovskite, the specific peaks are fit well with the standard card (PDF#: 28–0517) of $La_2Ti_2O_7$, illustrated the successful synthesized processes. It can be noticed that $La_2Ti_2O_7$ own a stacked sheet layer structure (Fig. 1B), which could provide large of active sites to fix other functional materials. Fig. 1C exhibits the XRD image of Sb_2S_3 and Cd: Sb_2S_3, the results prove that these two materials were all succeed in preparation, and the peaks strength were got stronger after Cd element doping, that means the crystal structure of the material is become better. As can be seen from Fig. 1D, the Cd: Sb_2S_3 has the fusiform structure, and the size is about in a 70 nm length and 30 nm width, TEM image of Cd: Sb_2S_3 is shown in Fig. S2A (in SM file). The mapping image in Fig. S2B, and XPS image in Fig. S2C also illustrated that Cd was successfully doped, and the original lattice structure of Sb_2S_3 was not destroyed. Fig. S3A shows the XPS data of Cd, two characteristic peaks were analyzed at 404.6eV and 411.4 eV, designated as Cd $3d_{5/2}$ and Cd $3d_{3/2}$, respectively, stating the Cd^{2+} state (Zhang et al., 2018a; Zhou et al., 2018). The XPS spectrum of Sb 3 d is shown in Fig. S3B. The peaks observed at 529.9 eV and 539.3 eV correspond to Sb $3d_{5/2}$ and Sb $3d_{3/2}$ (Peng et al., 2020; Sharma and Basu, 2021; Yang et al., 2020). These characteristic peaks are all indicate the Sb^{3+} state. Fig. S4 shows the SEM image of Cd: $Sb_2S_3/La_2Ti_2O_7$ composites. The XRD image of V_2O_5 is explained the triumphant preparation of V_2O_5 (Fig. 1E), resulting in a uniform nanosphere structure with a diameter size of about 100 nm (Fig. 1F).

3.2. Optimization of measurement conditions

For the sake of acquiring the best detection performance, it is necessary to optimize the experimental measurement conditions, and the electrolyte solution is the most important influencing factor for PEC testing. Thus, the pH environment of the PBS buffer solution, and the concentration of electron donor (H_2O_2) which was contained in PBS solution were considered to optimized. Fig. 2A shows the results of pH optimization, the PEC response reached the maximum value at pH 7.4, and also the photocurrent achieved the most stable state (Fig. S5A). While Fig. 2B shows the PEC performance achieved the best status when the concentration of H_2O_2 was 5 mM. As the concentration of H_2O_2 continues to increase, the photocurrent decreased. The possible reason is the saturation of the electron donor, which quenches the absorbance of the electrolyte solution, thereby reducing the light intensity and formation efficiency of the excited electron hole center, causing a negative impact on the photocurrent (Zhu et al., 2017), and the corresponding photocurrent value is shown in Fig. S5B. Therefore, a pH of 7.4 and a H_2O_2 concentration of 5 mM were selected as the test environment for the electrolyte PBS solution.

3.3. Electron transfer mechanism discussion

The possible PEC electrons transfer mechanism is shown in Scheme 2. Perovskite $La_2Ti_2O_7$ as one kind of potential photoactive materials provide a stable and better photocurrent after Au fabrication on the ITO surface (Fig. S6A). Sb_2S_3 nanoparticles act as functional photosensitizer was used to form heterojunction with $La_2Ti_2O_7$, and the matched band energy between these two materials further enhancing the photocurrent. Furthermore, the doping of Cd element preferred the band gap structure of Sb_2S_3 to a certain degree, and the narrow energy level gradient exhibited higher PEC performance (Fig. S6B). Scheme 2A displays the electron transfer process for PEC signal-on state, the presence of H_2O_2

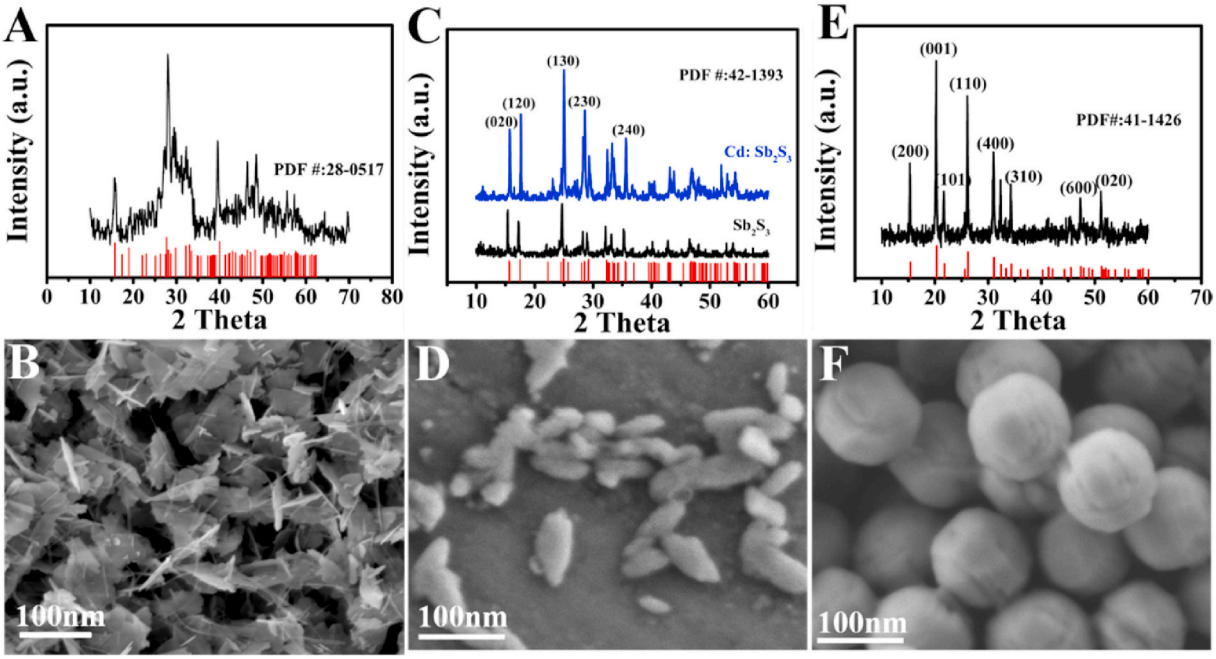

Fig. 1. XRD image (A) and SEM image (B) of $La_2Ti_2O_7$ nanosheet. XRD image (C) and SEM image (D) of Cd: Sb_2S_3. XRD image (E) and SEM image (F) of V_2O_5 nanosphere.

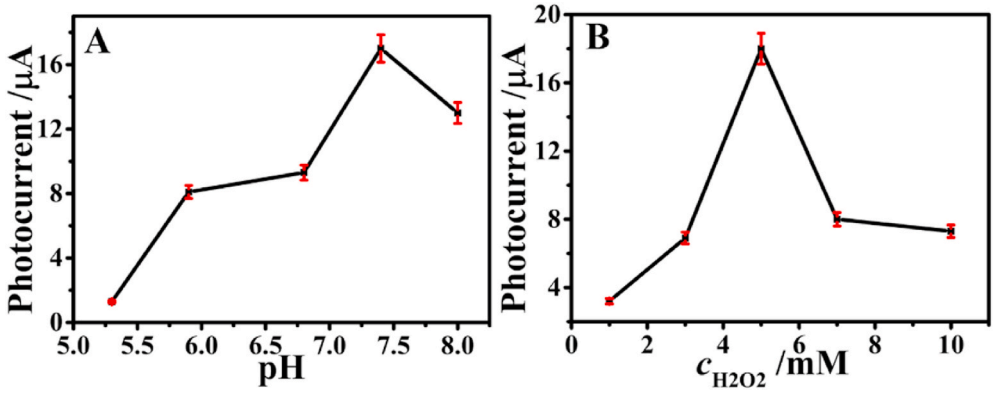

Fig. 2. The effect of pH (A) and concentration of H_2O_2 (B) for target detection. (c_{PSA} = 0.050 ng/mL). Error bars = SD (n = 3).

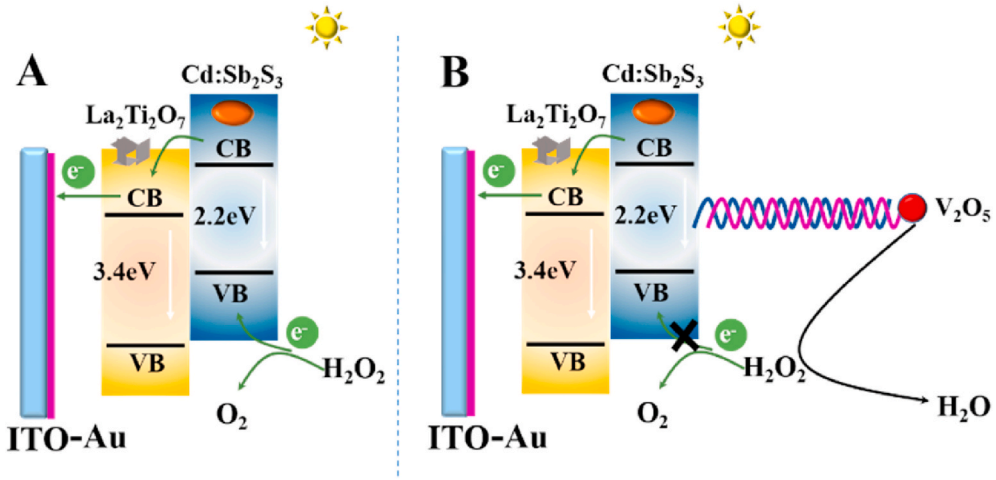

Scheme 2. Electron transfer mechanism (A) signal-on state and (B) signal-off state.

can further accelerated electron transfer. After modified the aptamer cDNA and aDNA-V_2O_5, the electrons would be impeded owing to the great steric hindrance of the non-conductive biomolecules. At the same time, V_2O_5 is an ideal catalyst to catalyze H_2O_2, and after the modification of V_2O_5, the concentration of H_2O_2 is greatly reduced, thus, the photocurrent decreased sharply through this process (Scheme 2B). Finally, various concentrations of analyst were decorated on the PEC aptasensor, part of aDNA-V_2O_5 could be specific recognized PSA and released from the sensor, then a PEC signal-on state was occurred again.

3.4. Sensor construction characterization

In order to acquire precisely and credible consequence, whether the designed PEC aptasensor is constructed successfully should be characterized. It is an intuitive way to detect the electrochemical performance of the sensor during the layer-by-layer modification. Fig. 3A shows the electrochemical impedance spectroscopy (EIS) image of the sensor fabrication processes. Pure ITO electrode owns a small impedance (curve a), after Au electrodeposition, a smaller impedance value was noticed (curve b) due to the excellent conductivity of noble metal. Then,

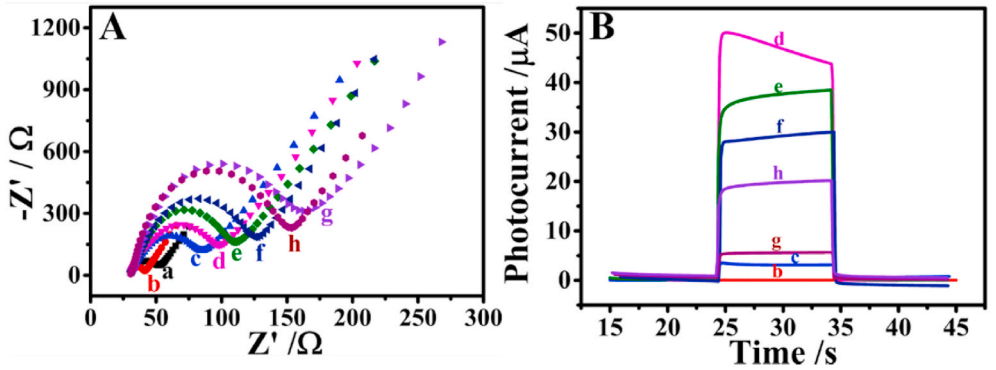

Fig. 3. The performance characterization of the PEC aptasensor. (A) EIS image and (B) photocurrent image. (a) ITO, (b) ITO-Au, (c) ITO-Au/$La_2Ti_2O_7$, (d) ITO-Au/$La_2Ti_2O_7$/Cd: Sb_2S_3, (e) ITO-Au/$La_2Ti_2O_7$/Cd: Sb_2S_3/EDC-NHS/cDNA, (f) ITO-Au/$La_2Ti_2O_7$/Cd: Sb_2S_3/EDC-NHS/cDNA/MCH, (g) ITO-Au/$La_2Ti_2O_7$/Cd: Sb_2S_3/EDC-NHS/cDNA/MCH/cDNA-V_2O_5 , (h) ITO-Au/$La_2Ti_2O_7$/Cd: Sb_2S_3/EDC-NHS/cDNA/MCH/cDNA-V_2O_5/PSA. (c_{PSA} = 0.050 ng/mL).

$La_2Ti_2O_7$ and Cd: Sb_2S_3 were decorated on the electrode step by step, the gradually increased impedance was obtained (curve c and d) because of the semi-conductivity. After that, the non-conductivity molecules of cDNA (curve e), MCH (curve f), aDNA-V_2O_5 (curve g) were decorated, and the resistance value was further enhanced. Finally, while target PSA was modified, a part of aDNA-V_2O_5 was specific recognized with antigen and released from the electrode, thus, a decreased resistance value was realized (curve h). The EIS value proved that the PEC aptasensor was successfully achieved.

As another and the most important electrochemical performance, photocurrent was measured during the layer-by-layer modification. As displayed in Fig. 3B, Au deposited ITO electrode has a nearly zero PEC response (curve b), after decorated the photoactive materials, the increased photocurrent was observed (curve c and d). Then, non-conductive molecules of cDNA (curve e), MCH (curve f), and aDNA-V_2O_5 (curve g) were dropped on the photosensitive surface, the photocurrent was decreased layer by layer, and because of the double quenching effect, the photocurrent attenuation was particularly obvious after aDNA-V_2O_5 modification. Finally, with the modification of PSA, the increased photocurrent occurred again thanks to the released of V_2O_5. It thus appears that the PEC sensor was constructed excitingly.

3.5. Target analysis

Under the preferred detection environment, the performance of PSA analysis is executed to realize the worth of sensor construction. It can be noticed that the PEC signal is enhanced with the concentration of PSA increasement (Fig. 4A), owing to the cumulative released of V_2O_5. The increased photocurrent has a linear relationship with concentration of PSA from 1.0×10^{-5} to 500.0 ng/mL, and the linear equation is $I = 20.05 + 2.562 \log c$ (ng/mL) (Fig. 4B). This super-sensitivity PEC aptasensor also own a low detection limit with 4.300 fg/mL which was calculated according to IUPAC36 (Long and Winefordner, 2012). The comparation of this sensor and other electrochemical methods is shown in Table S1.

3.6. Performance analysis of the PEC aptasensor

Analysis of the detection performance of the constructed sensor is the master key to ensuring the accuracy of the actual sample detection. Stability, reproductivity, and selectivity of the sensor were considered in this work before real sample detection. Fig. 5A shows the stability results of the sensor, it is observed that the sensor also remains stationary photocurrent after dozens of test loop. The storage lifetime analysis was also performed to characterize the storage stability of the sensor, and the results are shown in the revised Fig. S7. As can be seen form Fig. S7, and after two weeks, the signal was still remained 85 % of the original response, which means the sensor can still reach considerable detection standards after two weeks of storage. The reproducibility analysis of the sensor was performed by testing the photocurrent of six different electrodes which modified under the same conditions, Fig. 5B displays the satisfactory consequence of the reproductivity, and the RSD is 3.2 %. Selectivity is an effective means to characterize the anti-interference ability of sensors. In this study, BNP, Aβ, and PCT were selected as the interferences, which were modified with PSA on the electrode. The concentration of these interferences was 50-fold higher than PSA, and the detection results is shown in Fig. 5C, regardless of the presence or absence of PSA, the RSD of the selectivity measurement is below 6.0 %, certifying the great selectivity of the designed sensor. These detection results are all proving the exciting performance of the PEC aptasensor.

3.7. Real samples analysis

The real sample analysis was assessed the recovery in various concentrations (0.05, 0.5, 5, 50 ng/mL) of standard PSA solution which were added into the negative real serum sample (obtained from the hospital in University of Jinan). Table 1 shows the analysis results, the gratifying recovery rate ranges from 98 % to 104 %, and the RSD ranges from 3.3 % to 4.4 %. This satisfactory result explains the great potential application in real sample detection.

4. Conclusion

In conclusion, this work successfully constructed an ultra-sensitive PEC aptamer sensor based on the signal "on-off-on" strategy. The great fusiform-like Cd: Sb_2S_3 was effectively sensitized photoactive perovskite $La_2Ti_2O_7$, the formation of a heterojunction between these two materials greatly increased the PEC signal. V_2O_5 nanospheres with favorable catalytic properties was used as the marker labelled on aDNA, the steric effect and catalytic effect of V_2O_5 make the PEC signal decreased sharply. The last modified PSA will be specifically recognized by aDNA, and V_2O_5 was released from the electrode, thus, the PEC "signal-on" state occurred again. This skillful strategy not only improve the sensitivity of the sensor, but also widen the application of perovskite-kind of materials in PEC analysis field. Also, the designed sensor provides a referable mode for other target detection in analytical electrochemical territory.

Declaration of competing interest

The authors declare that they have no known competing financial interests or personal relationships that could have appeared to influence

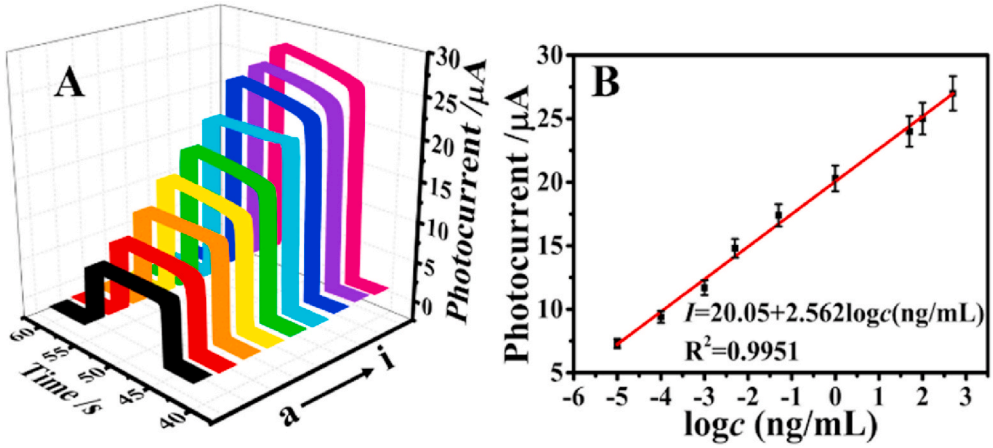

Fig. 4. The analytic performance of the target PSA. (A) PEC calibration curve of different concentrations. (a–i): 1.000×10^{-5}, 1.000×10^{-4}, 1.000×10^{-3}, 5.000×10^{-3}, 5.000×10^{-2}, 1.000, 50.00, 100.0, 500.0 ng/mL, and (B) linear relationship of the sensor. Error bars = SD (n = 3).

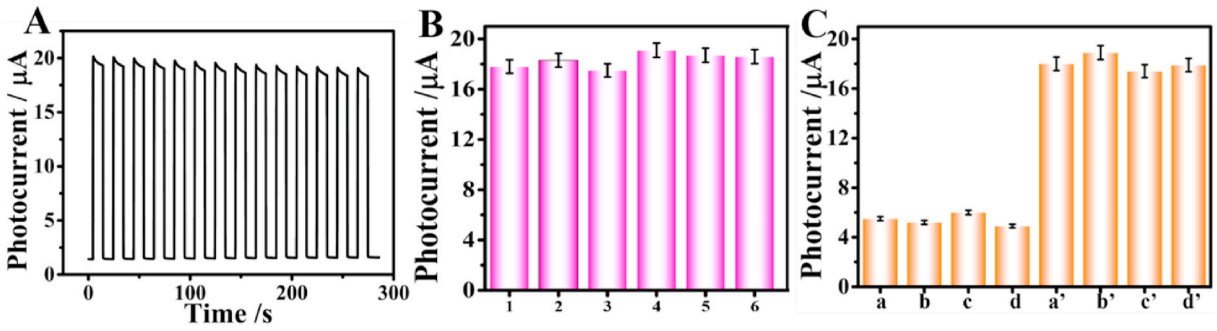

Fig. 5. Stability(A), reproductivity (B), and selectivity (C) detection of the sensor. The selectivity detection was performed without PSA (a) blank, (b) blank + BNP, (c) blank + Aβ, (d) blank + PCT, and in the present of PSA (a') PSA, (b') PSA + BNP, (c') PSA + Aβ, (d') PSA + PCT. (c_{PSA} = 0.050 ng/mL). Error bars = SD (n = 3).

Table 1
Recovery results of PSA in real samples detected by the proposed PEC sensor (n = 5).

sample	Added (ng/mL)	Found (average) (ng/mL))	Recovery (%)	RSD (%)
1	0.05	0.04910	98	3.3
2	0.5	0.5122	102	4.0
3	5	5.206	104	4.4
4	50	48.98	98	3.9

the work reported in this paper.

Acknowledgements

This item was subsidized by the National Key Scientific Instrument and Equipment Development Project of China (No. 21627809), National Natural Science Foundation of China (No. 21777056), Special Foundation for Taishan Scholar Professor-ship of Shandong Province, Jinan Scientific Research Leader Workshop Project (2018GXRC024, 2018GXRC021), and the Innovation Team Project of Colleges and Universities in Jinan (No.2019GXRC027).

Appendix A. Supplementary data

Supplementary data to this article can be found online at https://doi.org/10.1016/j.bios.2021.113528.

Author contribution

Rui Xu: Conceptualization, Data curation, Writing – original draft. Yu Du: Methodology, Data curation. Hongmin Ma: Methodology, Writing – review & editing. Dan Wu: Methodology, Writing – review & editing. Xiang Ren: Methodology, Data curation. Xu Sun: Writing – review & editing. Qin Wei: Supervision, Funding acquisition, Formal analysis. Huangxian Ju: Formal analysis.

References

André, R., Natálio, F., Humanes, M., Leppin, J., Heinze, K., Wever, R., Schröder, H.C., Müller, W.E.G., Tremel, W., 2011. Adv. Funct. Mater. 21 (3), 501–509.
Bin Adnan, M.A., Arifin, K., Minggu, L.J., Kassim, M.B., 2018. Int. J. Hydrogen Energy 43 (52), 23209–23220.
Chen, D., Liu, Z., Zhou, M., Wu, P., Wei, J., 2018. J. Alloy. Compd 742, 918–927.
Ghosh, S., Roy, P., Karmodak, N., Jemmis, E.D., Mugesh, G., 2018. Angew Chem. Int. Ed. Engl. 57 (17), 4510–4515.
Hu, Y.-L., Liu, X.-B., Fang, D., 2014. Catal. Sci. Technol. 4 (1), 38–42.
Huang, J., Zhang, L., Liang, R.P., Qiu, J.D., 2013. Biosens. Bioelectron. 41, 430–435.
Huang, L., Deng, H., Zhong, X., Zhu, M., Chai, Y., Yuan, R., Yuan, Y., 2019. Biosens. Bioelectron. 145, 111702.
Huang, L., Zhang, L., Yang, L., Yuan, R., Yuan, Y., 2018. Biosens. Bioelectron. 104, 21–26.
Huang, Y., Li, L., Zhang, Y., Zhang, L., Ge, S., Li, H., Yu, J., 2017. ACS Appl. Mater. Interfaces 9 (38), 32591–32598.
Kong, Q., Cui, K., Zhang, L., Wang, Y., Sun, J., Ge, S., Zhang, Y., Yu, J., 2018. Anal. Chem. 90 (19), 11297–11304.
Li, M., Zheng, Y., Liang, W., Yuan, Y., Chai, Y., Yuan, R., 2016. Chem. Commun. 52 (52), 8138–8141.
Liang, J., Chen, D., Yao, X., Zhang, K., Qu, F., Qin, L., Huang, Y., Li, J., 2020. Small 16 (15), e1903398.
Liu, X.P., Xie, X.L., Wei, Y.P., Mao, C.J., Chen, J.S., Niu, H.L., Song, J.M., Jin, B.K., 2017. Mikrochim. Acta 185 (1), 52.
Long, G.L., Winefordner, J.D., 2012. Anal. Chem. 55 (7), 712A–724A.
Lu, X., Liu, Z., Zhao, L., 2017. J. Sol. Gel Sci. Technol. 82 (1), 157–166.
Nassar, I.M., Wu, S., Li, L., Li, X., 2018. Chemistry 3 (3), 968–972.
Peng, Y., Chen, J., Jiang, L.-x., Wang, T.-y., Yang, H.-c., Liu, F.-y., Jia, M., 2020. Trans. Nonferrous Met. Soc. 30 (6), 1625–1634.
Ruan, Y.F., Zhang, N., Zhu, Y.C., Zhao, W.W., Xu, J.J., Chen, H.Y., 2017. Anal. Chem. 89 (15), 7869–7875.
Sharma, S., Basu, S., 2021. J. Clean. Prod. 280.
Tang, R., Wang, X., Jiang, C., Li, S., Liu, W., Ju, H., Yang, S., Zhu, C., Chen, T., 2018. ACS Appl. Mater. Interfaces 10 (36), 30314–30321.
Wan, S., Qi, F., Jin, W., Guo, X., Liu, H., Zhao, J., Zhang, J., Tang, C., 2018. J. Alloy. Compd 740, 901–909.
Wang, B., Cao, J.-T., Dong, Y.-X., Liu, F.-R., Fu, X.-L., Ren, S.-W., Ma, S.-H., Liu, Y.-M., 2018. Chem. Commun. 54 (7), 806–809.
Wang, C., Yang, S., Chen, X., Wen, T., Yang, H.G., 2017a. J. Mater. Chem. 5 (3), 910–913.
Wang, F., Li, W., Gu, S., Li, H., Liu, X., Ren, C., 2017b. Catal. Commun. 96, 50–53.
Wang, J., Shen, M., Cao, Y., Li, G., 2010. Biosens. Bioelectron. 26 (2), 638–642.
Wang, W., Xu, M., Xu, X., Zhou, W., Shao, Z., 2019. Angew. Chem. Int. Ed. 59 (1), 136–152.
Yang, F., Jiang, X., Zhong, X., Wei, S., Yuan, R., 2018. Sens. Actuators B-Chem. 265, 126–133.
Yang, K., Tang, J., Liu, Y., Kong, M., Zhou, B., Shang, Y., Zhang, W.H., 2020. ACS Nano 14 (5), 5728–5737.
Ye, C., Wang, M.Q., Luo, H.Q., Li, N.B., 2017. Anal. Chem. 89 (21), 11697–11702.
Zhang, K., Fujitsuka, M., Du, Y., Majima, T., 2018a. ACS Appl. Mater. Interfaces 10 (24), 20458–20466.
Zhang, L., Tian, Q., Lin, L., Li, J., 2019. Anal. Bioanal. Chem. 411 (18), 4041–4048.
Zhang, Z., Wu, L., Wang, P., Zhang, Y., Wan, S., Guo, X., Jin, W., Zhang, J., 2018b. Mater. Lett. 230, 72–75.
Zhou, M., Wang, S., Yang, P., Huang, C., Wang, X., 2018. ACS Catal. 8 (6), 4928–4936.
Zhu, H., Yan, S., Li, Z., Zou, Z., 2017. ACS Appl. Mater. Interfaces 9 (39), 33887–33895.
Zhu, M., Zhong, X., Deng, H., Huang, L., Yuan, R., Yuan, Y., 2019. Biosens. Bioelectron. 143, 111618.
Zou, M., Wen, W., Li, J., Lai, H., Huang, Z., 2016. J. Alloy. Compd 681, 268–274.